AGU PUBLICATIONS

Water Resources Research

RESEARCH ARTICLE
10.1002/2017WR021234

Key Points:
- Travel times of hydraulic fracturing fluid back to near surface aquifers on the order of 10,000 years
- High hydraulic conductivity formations can be more effective vertical fluid flow barriers than low hydraulic conductivity formations
- Low hydraulic conductivity faults can encourage vertical fluid flow by developing subsurface pressure compartmentalization

Correspondence to:
M. Wilson,
miles.wilson@durham.ac.uk

Citation:
Wilson, M. P., Worrall, F., Davies, R. J., & Hart, A. (2017). Shallow aquifer vulnerability from subsurface fluid injection at a proposed shale gas hydraulic fracturing site. *Water Resources Research*, *53*. https://doi.org/10.1002/2017WR021234

Received 2 JUN 2017
Accepted 7 NOV 2017
Accepted article online 10 NOV 2017

Shallow Aquifer Vulnerability From Subsurface Fluid Injection at a Proposed Shale Gas Hydraulic Fracturing Site

M. P. Wilson[1], F. Worrall[1], R. J. Davies[2], and A. Hart[3]

[1]Department of Earth Sciences, Durham University, Science Labs, Durham, UK, [2]School of Natural and Environmental Sciences, Newcastle University, Newcastle, UK, [3]Environment Agency, Research Assessment and Evaluation, Solihull, UK

Abstract Groundwater flow resulting from a proposed hydraulic fracturing (fracking) operation was numerically modeled using 91 scenarios. Scenarios were chosen to be a combination of hydrogeological factors that a priori would control the long-term migration of fracking fluids to the shallow subsurface. These factors were induced fracture extent, cross-basin groundwater flow, deep low hydraulic conductivity strata, deep high hydraulic conductivity strata, fault hydraulic conductivity, and overpressure. The study considered the Bowland Basin, northwest England, with fracking of the Bowland Shale at ~2,000 m depth and the shallow aquifer being the Sherwood Sandstone at ~300–500 m depth. Of the 91 scenarios, 73 scenarios resulted in tracked particles not reaching the shallow aquifer within 10,000 years and 18 resulted in travel times less than 10,000 years. Four factors proved to have a statistically significant impact on reducing travel time to the aquifer: increased induced fracture extent, absence of deep high hydraulic conductivity strata, relatively low fault hydraulic conductivity, and magnitude of overpressure. Modeling suggests that high hydraulic conductivity formations can be more effective barriers to vertical flow than low hydraulic conductivity formations. Furthermore, low hydraulic conductivity faults can result in subsurface pressure compartmentalization, reducing horizontal groundwater flow, and encouraging vertical fluid migration. The modeled worst-case scenario, using unlikely geology and induced fracture lengths, maximum values for strata hydraulic conductivity and with conservative tracer behavior had a particle travel time of 130 years to the base of the shallow aquifer. This study has identified hydrogeological factors which lead to aquifer vulnerability from shale exploitation.

1. Introduction

Hydraulic fracturing (fracking) is a process used to recover commercial quantities of oil and gas from low permeability unconventional reservoirs such as shale. Pressurised fluid, usually consisting of water, chemical additives, and a proppant (e.g., sand) is injected via a borehole into low permeability rock to induce hydraulic fractures. These fractures, kept open by the proppant, increase the permeability of the rock and allow oil and gas to flow back to the surface via the borehole. While the technology of fracking has been used for decades, its widespread use to exploit shale reservoirs with multiple stages in horizontal boreholes is a more recent development (King, 2012). The United States of America (USA) increased shale gas production through fracking from 1,293 billion cubic feet (bcf) in 2007 to 15,213 bcf in 2015 (US EIA, 2016). Conversely, England is still in the exploratory stage with uncertain resource estimates (e.g., Andrews, 2013). To date only one borehole targeting shale gas, Preese Hall 1 in Lancashire, has been fracked in England. In England environmental protection related to shale exploitation, which includes groundwater protection, waste management, and assessment of chemicals intended for use in fracking, is governed by a range of existing regulations plus additional local controls under the planning system.

The environmental impacts of fracking for shale gas and oil have been a global topic of discussion (e.g., Brownlow et al., 2017; Clancy et al., 2017; Davies et al., 2013, 2014; Kahrilas et al., 2014; Vengosh et al., 2013). One environmental concern is the potential risk of groundwater contamination from the fluids used in the fracking process (EA, 2013). A particular question is whether fracking fluids injected into the subsurface at depths of several kilometers can migrate via natural geological pathways to shallow aquifers at depths of tens to hundreds of meters (Figure 1). In the Marcellus shale play, USA, the deepest reported drinking-water level is ~600 m below the surface (Fisher & Warpinski, 2012). Similarly, groundwater abstractions in England typically do not descend more than 200 m below ground level and it has been suggested that a reasonable

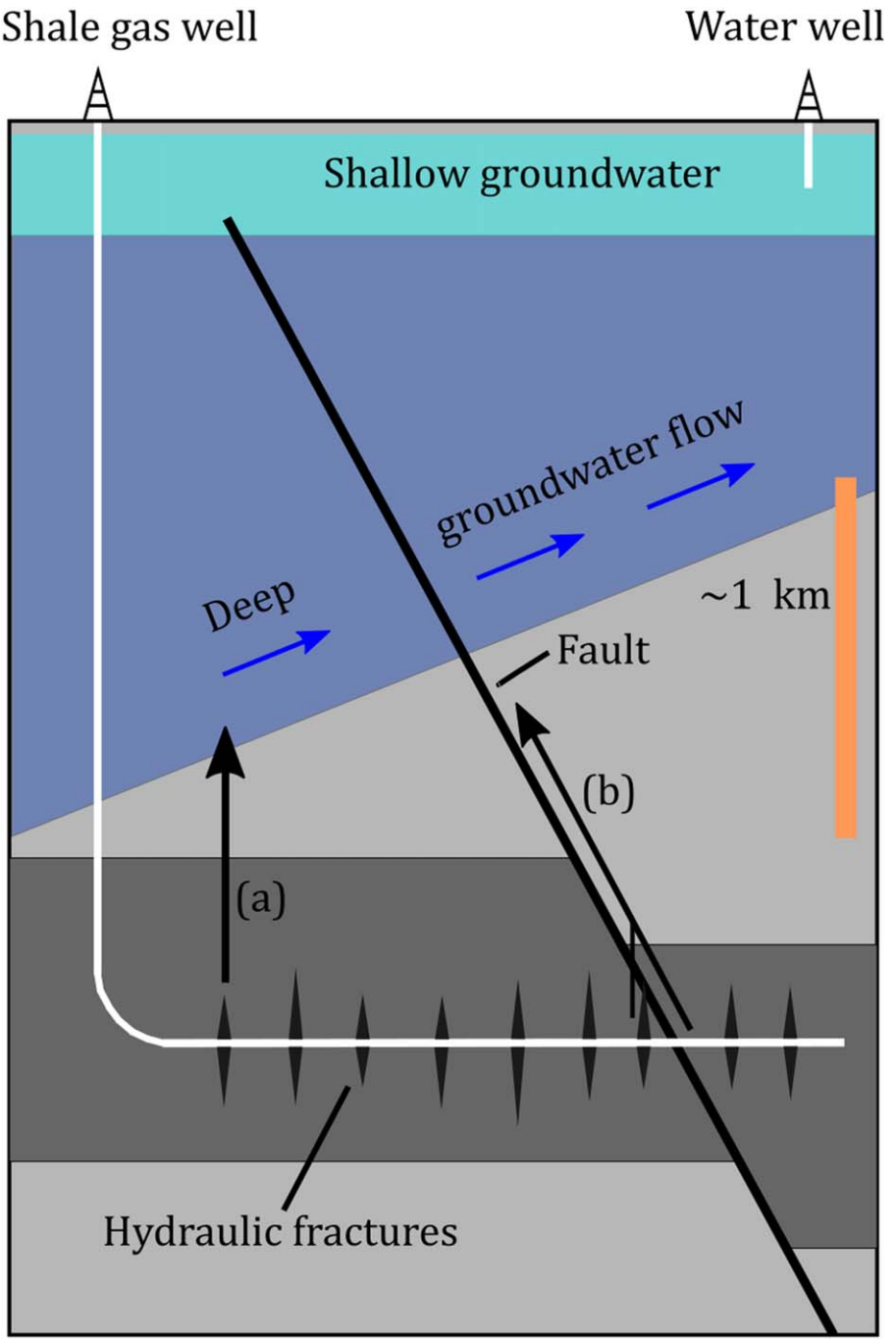

Figure 1. Schematic diagram showing potential natural geological pathways for fracking fluids to migrate to shallow aquifers. (a) Induced fractures providing an entry point to strata which are hydrologically connected to shallow aquifers. (b) Induced fractures or borehole perforations connecting to a high hydraulic conductivity fault.

maximum depth of ~400 m may be considered for conventional freshwater aquifers (UKTAG, 2011). English regulations ensure that fracking only occurs 1,000 m below the surface and 1,200 m below the surface in: specified groundwater areas, National Parks, Areas of Outstanding National Beauty, and World Heritage Sites. Considering that Davies et al. (2012) reported a maximum observed induced fracture height of ~588 m and a ~1% probability of an induced fracture exceeding 350 m, it is unlikely that induced fractures would directly connect stimulated shale zones to shallow aquifers (Flewelling & Sharma, 2014). However, it is possible that if induced fractures provided an entry point to strata that are sufficiently hydrologically

connected to shallow aquifers, upward migration of injected fluid could occur under certain hydraulic conditions (Figure 1).

A further possible natural fluid pathway to shallow aquifers exists if induced fractures or borehole perforations directly link to high hydraulic conductivity (i.e., high permeability) geological faults that extend to the shallow subsurface (Figure 1). Such a scenario would require particular hydraulic gradients and the fault to be highly conductive along its length. Hydraulic conductivity can vary greatly from fault to fault (e.g., Seymour et al., 2006) and also along a single fault (e.g., Fisher & Knipe, 2001), thereby complicating flow prediction. Boothroyd et al. (2017) indicated that basin-bounding faults in England, including some in shale gas basins, can act as conduits for methane to travel from the deep subsurface to the surface without anthropogenic disturbance. Fracking operations in England must avoid major faults because of concerns related to induced seismicity (Green et al., 2012; Wilson et al., 2015). It is therefore unlikely, although still possible, that induced fractures or borehole perforations would directly link with known basin-bounding faults.

Observed subsurface groundwater contamination from fracking sites is rare and disputed. It is usually thought to be associated to well casing integrity issues or surface leaks (e.g., DiGiulio et al., 2011; Llewellyn et al., 2015; Wright et al., 2012) and not from the migration of fracking fluids from the deep to shallow subsurface along natural geological pathways. To assess the latter issue, field-based groundwater monitoring can be undertaken, but this requires baseline conditions to be known and tens of years of monitoring. A more practical short-term solution is numerical modeling. Myers (2012) produced the first numerical model to assess upward fluid migration from fracking. Fracking fluid was reported to reach aquifers within 10 years (Myers, 2012). However, the model was criticized due to unrealistic geology (e.g., Cohen et al., 2013). Gassiat et al. (2013) produced a more realistic model using global shale basin data to assess the potential for upward fluid migration along conductive faults. Model results for a scenario with fracking at ~1,800 m below the surface indicated a 500 year travel time to a depth of 500 m below the surface (Gassiat et al., 2013). Kissinger et al. (2013) also investigated upward fluid flow from fracking but instead focused on the Münsterland and Lower-Saxony Basins, Germany. Three scenarios were designed to cover the migration of fracking fluids, brine, and methane on local and regional scales, as well as on short-term and long-term temporal scales. Results indicated that fluid migration to shallow layers can occur if a combination of assumptions are met, for example, the presence of high permeability fault zones which connect the stimulated shale and the aquifer (Kissinger et al., 2013). Cai and Ofterdinger (2014) modeled a nonfaulted hypothetical reference scenario for the Bowland Shale in Lancashire, England. Their worst-case scenario, with fractures directly connecting the fracked shale to the shallow aquifer, resulted in aquifer contamination in 100 years. Further, Palat et al. (2015) and Pfunt et al. (2016) investigated the effects of faults on fracking fluid migration using models of the North Perth Basin (Australia) and the North German Basin (Germany), respectively. Neither study observed fracking fluids reaching the regional aquifers within the simulated timescales of 20 and 300 years, respectively. Arguably the most advanced numerical model investigating fracking fluid migration is that by Birdsell et al. (2015). Birdsell et al. (2015) reviewed previous numerical models and identified that no model had combined the effects of buoyancy, well operations, and capillary imbibition. They constructed a numerical model to include these effects and various scenarios were run with sensitivity analyses. No fracking fluid was observed to reach the shallow aquifer when a permeable pathway (modeled as either a fault or borehole) was not present. When a permeable pathway was present the effect of well production and capillary imbibition were to reduce the amount of fracking fluid reaching the aquifer by a factor of ten.

Since Myers (2012) the complexity of numerical models investigating upward fluid flow from fracking operations has generally increased. However, one aspect that has remained relatively untouched is the inclusion of more complex geological structure; models to date have tended to use horizontal geological strata and homogenous overburdens to the shale reservoir. This can be appropriate for some sedimentary basins, but may not appropriate for more complex basins such as the Bowland Basin, northwest England. The aim of this numerical modeling study is to consider the hydrogeological factors within a complex sedimentary basin that would contribute to decreasing the travel time for fracking fluids injected at ~2,000 m depth to reach a shallow aquifer at ~300–500 m depth. These hydrogeological factors may increase or decrease how vulnerable the aquifer is to any type of contaminant at a particular locality (Palmer & Lewis, 1998; Worrall & Kolpin, 2004). This study is the first to use analysis of variance (ANOVA) to identify hydrogeological factors which play a statistically significant role in decreasing the fluid travel time between a fracked shale and shallow groundwater resources.

2. Approach and Methodology

In this study, a recently proposed fracking project in Lancashire, England, was numerically modeled (Figure 2). If this fracking project goes ahead it will target the Bowland Shale, an organic-rich shale deposited during the mid-Carboniferous across northern England (Andrews, 2013). This will be the first English fracking operation to target shale gas using a horizontal borehole.

Numerical modeling was performed using ModelMuse and MODFLOW. The model scenarios were selected to be a factorial combination of the hydrogeological factors of interest. The factors being considered were the presence of faults acting as conduits, the vertical extent of induced fractures, the presence of deep low hydraulic conductivity strata above the target shale formation, the presence of deep high hydraulic conductivity strata above the shale formation, cross-basin groundwater flow, and overpressure. Particle tracking was used to provide a measure of the fracking fluid travel time to the regional shallow aquifer. ANOVA was used to analyze the results.

The effects of faulting were a particular focus here because faults can act as conduits and barriers to regional groundwater flow. It is already known that faults influence shallow groundwater flow in the Lancashire area (Seymour et al., 2006). The effects of low and high hydraulic conductivity strata above the shale formation were considered as both have been suggested to act as barriers to vertical fluid migration (Ove

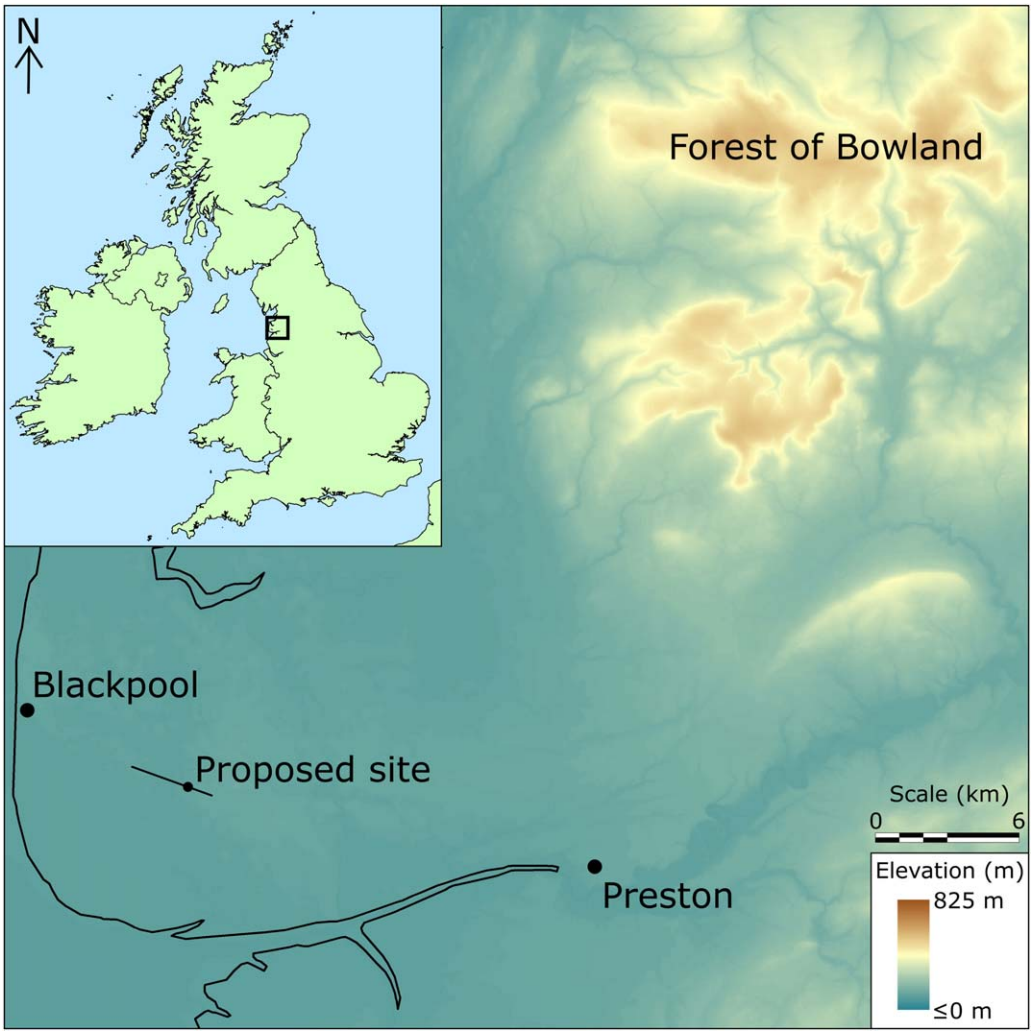

Figure 2. Location of the proposed fracking site and associated geological cross section of Figure 3a (solid black line). The black outlined box on the inset UK map shows the location of the enlarged map. Contains OS data © Crown copyright and database right (2016).

Arup and Partners Ltd., 2014a; Cai & Ofterdinger, 2014). While the analysis was undertaken on a specific site, we identify hydrogeological factors that could increase or decrease aquifer vulnerability across global shale basins.

2.1. MODFLOW, ModelMuse, and MODPATH

MODFLOW is an open-access finite-difference groundwater code created by the United States Geological Survey (USGS) (McDonald & Harbaugh, 1984). This study used the latest version; MODFLOW-2005. MODFLOW simulates steady and transient groundwater flow in irregularly shaped flow systems subject to external stresses such as wells, areal recharge, evapotranspiration, drains, and rivers (Harbaugh, 2005). MODFLOW has been used to model groundwater scenarios from small-scale localized fracking (e.g., Myers, 2012) to large-scale regional studies (e.g., Belcher & Sweetkind, 2010).

To build a hydrogeological model to run using MODFLOW, the USGS graphical user interface "ModelMuse" was used. ModelMuse enables the user to create a model grid and input spatial and temporal data such as hydrogeological parameters and boundary conditions (Winston, 2009). MODFLOW can be executed from ModelMuse and the results also displayed through ModelMuse. Within ModelMuse, the MODPATH Version 6 package was used to undertake particle tracking. MODPATH is a postprocessing particle tracking code which computes three-dimensional (3-D) groundwater flow paths using the output from MODFLOW groundwater flow simulations (Pollock, 2012). Particle tracking provided a prediction of the long-term migration route of injected fracking fluid and travel time to the shallow aquifer.

2.2. Geological Model

The geological model included folded and dipping strata, strata thickness variations, erosional truncation geometries, and faulting. A schematic geological cross section for the expected geology and structural features at the proposed fracking site was provided in the submitted Environmental Statement required for the development (Ove Arup and Partners Ltd. 2014a). This cross section is orientated approximately west-northwest to east-southeast and has approximate dimensions of 3.5 by 3.7 km^2 (Figure 3a). A single borehole trajectory is shown contained within the Upper Bowland Shale. The predicted strata were modified to account for the commonly observed two-layer stratification of the Sherwood Sandstone Group; the upper more hydraulically conductive Sherwood Sandstone and the lower, less hydraulically conductive St. Bees Sandstone (Allen et al., 1997; Ambrose et al., 2014). The Sherwood Sandstone forms Lancashire's primary regional aquifer in the east Bowland Basin (Allen et al., 1997).

The Haves Ho fault is interpreted to extend from the Hodder Mudstone (the underlying formation to the Bowland Shale) to the surface (Figure 3a) (Ove Arup and Partners Ltd. 2014b). Due to this possible direct conduit to the surface, the study cross section and modeled area were extended westward (6.0 by 3.5 km^2, with grid spacing of 50 by 50 m^2 as shown in Figure 4), ensuring the geological model was consistent with the seismic reflection interpretations of the Haves Ho fault shown by Ove Arup and Partners Ltd. (2014b) (Figure 3b). A result of this is the lithological change in the bottom left corner of the cross section.

2.3. Hydrogeological Models

The typical strata hydraulic properties identified by Cai and Ofterdinger (2014) were used to populate the geological model (Table 1). No hydraulic distinction was made between the Upper and Lower Bowland Shales because one-way ANOVA of core plug permeability data (restricted access so not shown) from the Preese Hall 1 borehole (Hird & Clarke, 2012) showed that measured values were not statistically different between the stratigraphically defined Upper and Lower Bowland Shale. The numbers of measured core plug samples were: 13 horizontal and 5 vertical permeabilities from the Upper Bowland Shale and 8 horizontal and 2 vertical permeabilities from the Lower Bowland Shale. The formation (Upper or Lower) and permeability direction (horizontal or vertical) had probabilities of having zero effect of 0.756 and 0.659, respectively.

Above the Bowland Shale there are two formations of particular interest. First, the Manchester Marl (Figure 3a) is a low hydraulic conductivity formation that has been proposed as protecting the overlying aquifer from ingress of fracking fluids (Ove Arup and Partners Ltd., 2014a). Second, the Collyhurst Sandstone (Figure 3a) is a relatively high hydraulic conductivity layer at the base of the Permian sequence, which has also been proposed to protect the overlying aquifer from the ingress of any fracking fluids (Cai & Ofterdinger, 2014). In some modeled scenarios, the low hydraulic conductivity Manchester Marl, the high hydraulic

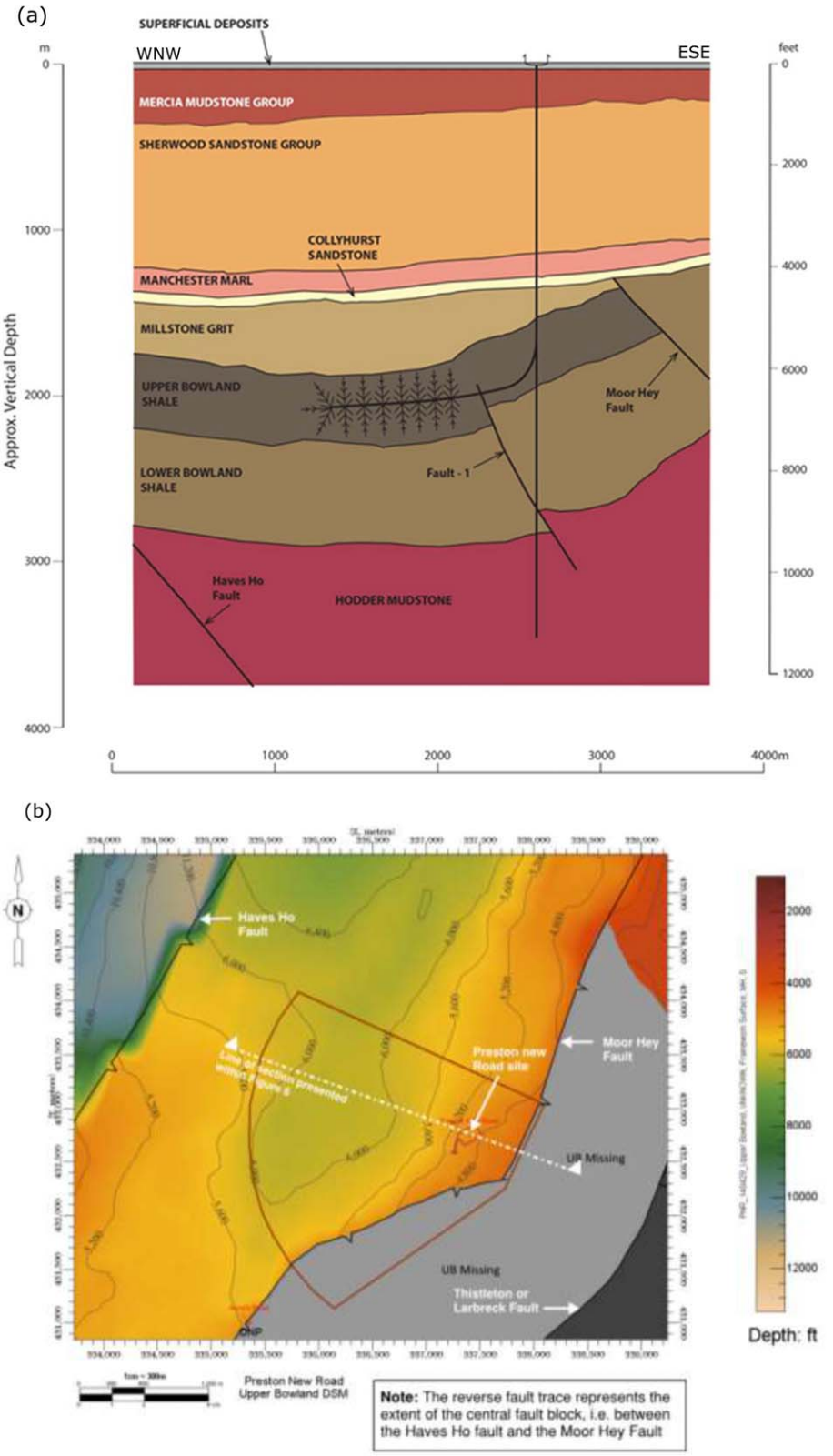

Figure 3. (a) Geological cross section of the expected geology and structure at the proposed fracking site. (b) Depth structure map illustrating the depth below ground level of the top of the Upper Bowland Shale. The locations of interpreted faults and the cross section of (a) (dashed white line) are also shown. Images adapted from Ove Arup and Partners Ltd. (2014b).

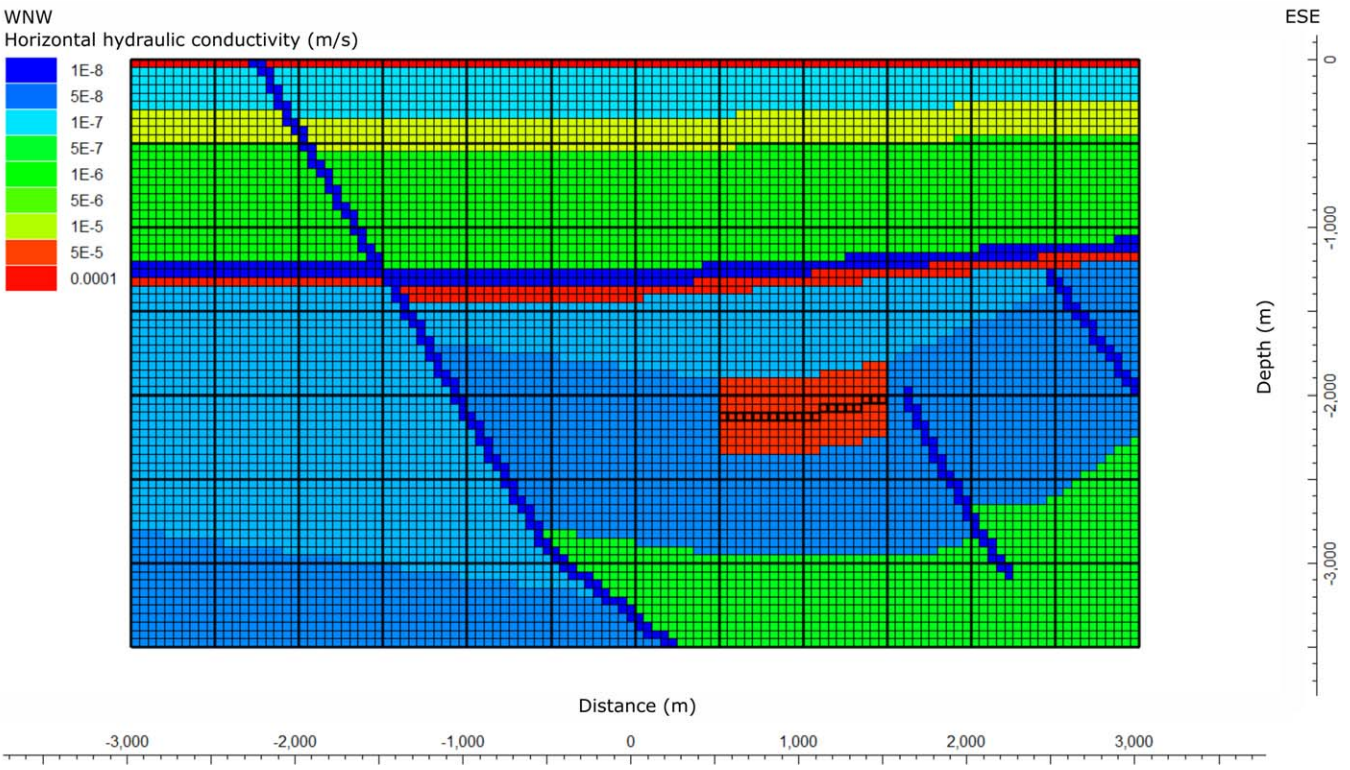

Figure 4. Hydrogeological model of Figure 3a, including predicted extension to the west-northwest. The finer grid spacing is 50 by 50 m^2. Fracking stages are shown as bold black outlined squares contained within an induced vertical fracture extent of 200 m above and below the stages (red).

conductivity Collyhurst Sandstone, or both formations were removed. The removal of the Manchester Marl was achieved by assigning this model layer the same hydraulic properties as the overlying St. Bees Sandstone. This approach was also taken when both formations were removed. The removal of the Collyhurst Sandstone was achieved by assigning this model layer the same hydraulic properties as the Manchester Marl. The removal of these formations was undertaken to investigate how potential fluid migration changes

Table 1
Hydraulic Parameters for Hydrogeological Model Scenarios

Unit	Horizontal hydraulic conductivity (K_h) (m s^{-1})	K_h/K_v	Fracked hydraulic conductivity (m s^{-1})	Porosity (fraction)	Storage coefficient (S_c)
Superficial Deposits	1.7×10^{-4}[a]	100,000[a]	n/a	0.30[b]	10^{-3}[b]
Mercia Mudstone Group	10^{-7}	100	n/a	0.10	10^{-3}
Sherwood Sandstone	1.2×10^{-5}	10	n/a	0.23	2.0×10^{-3}
St. Bees Sandstone	8.1×10^{-7}	10	n/a	0.15	8.6×10^{-5}
Manchester Marl	10^{-8}	10	n/a	0.15	2.0×10^{-5}
Collyhurst Sandstone	7.9×10^{-5}	10	n/a	0.26	5.0×10^{-4}
Millstone Grit	7.9×10^{-8}	10	7.9×10^{-5}	0.08	10^{-4}
Bowland Shale (Upper and Lower)	6.0×10^{-8}	10	6.0×10^{-5}	0.03	10^{-4}
Hodder Mudstone (formerly called the Worston Shales)	6.0×10^{-7}	10	n/a	0.03	10^{-4}
Faults (*Moor Hey Fault, Fault-1, Haves Ho Fault*)	10^{-12} (low)[c] 10^{-8} (medium) 10^{-4} (high)	1	n/a	Not modeled	Not modeled

Note. Data from Cai and Ofterdinger (2014) unless stated. "n/a" indicates not applicable.
[a]Based on Mott MacDonald's and the Environment Agency's conceptual model for the Fylde Aquifer.
[b]Assumed. Other values make negligible difference to simulation and particle tracking results.
[c]Low fault hydraulic conductivity is from a permeability of 10^{-19} m^2 (Rutqvist et al., 2013, 2015).

with their absence because their occurrence at the site has yet to be proven with drilling. Seismic interpretation in the Bowland Basin suggests that in some locations the Collyhurst Sandstone was not deposited (Clarke et al., 2014).

The hydraulic properties of the faults at the proposed site (Moor Hey Fault, Fault-1, Haves Ho Fault; Figure 3) are highly uncertain. These faults were therefore modeled with low, medium, and high estimates for hydraulic conductivity (Table 1). The low hydraulic conductivity case was taken as a fault permeability of 10^{-19} m^2 (Rutqvist et al., 2013, 2015) and converted to hydraulic conductivity by assuming gravitational acceleration of 10 m s^{-2} and fluid density and viscosity of 1,000 kg m^{-3} and 0.001 kg m^{-1} s^{-1}, respectively. The allocation of bulk hydraulic conductivity values to the fault zone grid blocks followed a similar approach to Gassiat et al. (2013), where a bulk permeability value was applied to the fault zone without considering fracture apertures and grid block size. More complex approaches do exist, such as the dual porosity and cubic law approach by Birdsell et al. (2015), but application to models with complex geological structure is much more difficult; our fault zones are inclined relative to the model grid and the shale overburden is inhomogeneous. The three fault scenarios represent cases where the faults have lower, similar or higher hydraulic conductivities relative to the surrounding strata. Each scenario assumes that all faults have the same hydraulic properties as each other and that these properties do not vary along the fault length. This is a simplification of reality but is a practical approach when further information does not yet exist for these faults.

All models include three stress periods: an initial 30 year steady state period, a 2 h transient fluid-injection period (no fluid injected in scenarios with no fracture propagation), and a 10,000 year transient-state period. To model an induced fracture network, the hydraulic conductivities of the strata immediately overlying and underlying the horizontal borehole were increased by a factor of 1,000 to represent the increase in hydraulic conductivity caused by stable induced fractures (Gaskari & Mohaghegh, 2006). The fractured areas in the models can be thought of as two-dimensional (2-D) representations of stimulated reservoir volumes (SRVs) (Mayerhofer et al., 2010). We make these hydraulic conductivity changes after the initial steady state period but prior to fluid injection. Due to software limitations, this approach required the initial steady state periods to be modeled as separate simulations and their outputs used as the starting conditions for the transient periods.

The fractured extents modeled were 0 (no fracking and fluid injection represents a natural groundwater flow scenario), 200, and 600 m above and below the borehole. The horizontal portion of the borehole is situated at ~2,000 m depth. An upper limit of 600 m was chosen because the largest reported vertically induced fracture in the Barnett Shale was found to be ~588 m (Davies et al., 2012). A 600 m extent results in fracture propagation into the overlying Millstone Grit. A 200 m fracture extent was also modeled because this extent reaches the upper boundary of the Bowland Shale at the proposed site, but does not penetrate the overlying Millstone Grit (Figure 4). It is hypothesized that the induced fractured extent will be ~50–150 m from the borehole (Ove Arup and Partners Ltd., 2014b). Due to the 2-D nature of the model, the lateral extent of horizontally induced fractures was not considered.

2.4. Boundary Conditions

Both the presence of a horizontal hydraulic head gradient (resulting in cross-basin groundwater flow) and the magnitude of overpressure were considered important factors in the study design. Two levels of horizontal hydraulic head gradient were considered. First, the same horizontal hydraulic head boundary condition as applied by Cai and Ofterdinger (2014) was applied to our model. A horizontal hydraulic head gradient of 0.5% was applied with flow from east-southeast to west-northwest (i.e., east-southeast boundary had a hydraulic head of 3,530 m and the west-northwest boundary 6,000 m away had a hydraulic head of 3,500 m). Groundwater is expected to flow from northeast/east to southwest/west (MacDonald, 1997), but due to the 2-D nature of the model domain the horizontal gradient was assigned as stated. Second, the horizontal hydraulic gradient was removed by applying a hydraulic head of 3,500 m to the east-southeast boundary.

Hydraulic heads of either 3,850 or 4,900 m were applied to the entire lower boundary of the model. The hydraulic head of 4,900 m corresponds to ~40% overpressure above hydrostatic pressure; the overpressure as measured at Preese Hall 1 (Cai & Ofterdinger, 2014). The hydraulic head of 3,850 m corresponds to a lower overpressure of 10%. Rainfall recharge was not assigned to the model upper boundary based on the

assumption that little rainfall recharge reaches deeper than the Mercia Mudstone. This assumption of no rainfall recharge at depth means that the horizontal head gradient was the result of recharge from the upgradient topography of the Forest of Bowland (Figure 2).

2.5. Fluid Injection and Particle Tracking

Details of the proposed injection of fluid are yet to be confirmed. This study considered a single 1,000 m long, strata-parallel borehole with injection stages at 50 m intervals (i.e., 20 stages) (Figure 4). Each stage within the model was represented as a point source using the Well package (WEL) within ModelMuse and MODFLOW. For simplification and consistent with Cai and Ofterdinger (2014), all stages were injected simultaneously at a rate of $\sim$0.35 $m^3\ s^{-1}$ for 2 h, equivalent to stage injection volumes of 2,500 m^3. Flowback and production volumes were not accounted for. The simultaneous injection without flowback and production can be thought of as a worst-case situation. In reality, flowback and production operations would occur between each stage, reducing the volume of fracking fluid left in the subsurface and also reducing the pore pressure. Flowback and production may reduce the risk of injected fluid migrating beyond the SRV. The neglect of flowback and production is discussed in section 4.6.3.

Particle tracking was used to investigate potential migration routes and travel times to the base of the Sherwood Sandstone (the primary regional aquifer). Because fracture propagation was not modeled explicitly, particle tracking was initiated at the furthest extent of the SRV and at the end of the two hour injection period. This approach assumes that injected fluid reaches the edges of the SRV, although it is unclear if this always occurs in practice. Again this is a worst-case assumption and is further discussed in section 4.6.2. Particles were tracked for 10,000 years after the termination of injection.

2.6. Scenario Design and Statistical Analysis

The scenario design used in this study was a factorial design with respect to the Manchester Marl, the Collyhurst Sandstone, a cross-basin horizontal head gradient, induced fracture extent, fault hydraulic conductivity, and overpressure. For the Manchester Marl, the Collyhurst Sandstone, and the horizontal hydraulic head gradient, only two levels were considered for each factor. These were the presence or absence of that stratum or phenomenon. For the induced fracture extent three levels (0, 200, and 600 m) were considered. Fault hydraulic conductivity also considered three levels (10^{-12}, 10^{-8}, and 10^{-4} m s^{-1}). The factorial combination resulted in 72 scenarios. A second factorial analysis was then used to investigate the influence of overpressure; two levels (10% and 40% above hydrostatic pressure) were used in conjunction with statistically significant factors from the previous 72 scenarios. Overall 91 scenarios were modeled.

ANOVA in Minitab (v.17) was used to assess the significance of individual factors and the two-way interactions between them, with significance judged at the 95% probability of the factor or interaction not having zero effect. Scenarios where particles did not reach the Sherwood Sandstone within 10,000 years were assigned an arbitrary travel time of 15,000 years. The Tukey test was used post hoc to assess where significance lay within factors with three levels. The factor and level effects are reported as least squares means (marginal means) as these are the best measure of the average after allowing for the influence of the other factors and interactions. The proportion of the variance explained by each factor and interaction was estimated using the ω^2 method of Olejnik and Algina (2003).

The hydraulic properties of the deep strata in the Lancashire area are uncertain. The factorial analysis did not consider the potential range of hydraulic conductivities for strata due to the large number of models and time this would require. Instead, a single worst-case scenario was modeled. This was achieved by using the maximum values for strata hydraulic conductivity used by Cai and Ofterdinger (2014) (see their Table 1) in the factorial scenario which resulted in the shortest particle travel time to the Sherwood Sandstone. The minimum, typical, and maximum hydraulic conductivity values used by Cai and Ofterdinger (2014) covered three orders of magnitude.

3. Results

Of the 72 scenarios modeled in the initial factorial analysis, 16 of these resulted in particles reaching the base of the Sherwood Sandstone within 10,000 years (Table 2). All of these 16 scenarios had the Collyhurst Sandstone absent. The shortest particle travel time to the Sherwood Sandstone was 560 years (expressed to the nearest 10 years), which occurred when the induced fractures were 600 m and the Manchester Marl,

Table 2
Factorial Scenarios That Resulted in Particle Travel Times Under 10,000 Years to the Base of the Sherwood Sandstone

Induced fracture extent (m)	Fault hydraulic conductivity (m s^{-1})	Manchester Marl present?	Collyhurst Sandstone present?	Horizontal head gradient present?	Travel time to nearest 10 years
200	10^{-8}	Yes	No	Yes	9,390
200	10^{-8}	Yes	No	No	7,430
200	10^{-8}	No	No	Yes	3,660
200	10^{-8}	No	No	No	3,200
600	10^{-8}	Yes	No	Yes	3,140
200	10^{-12}	Yes	No	Yes	3,050
200	10^{-12}	Yes	No	No	2,990
600	10^{-8}	Yes	No	No	2,900
200	10^{-12}	No	No	No	1,760
200	10^{-12}	No	No	Yes	1,720
600	10^{-12}	Yes	No	No	1,490
600	10^{-12}	Yes	No	Yes	1,460
600	10^{-8}	No	No	Yes	790
600	10^{-8}	No	No	No	790
600	10^{-12}	No	No	Yes	580
600	10^{-12}	No	No	No	560

Collyhurst Sandstone, and horizontal head gradient were absent. None of the scenarios without fracking and fluid injection resulted in particles reaching the Sherwood Sandstone within 10,000 years.

3.1. Factors

The factors of Collyhurst Sandstone, induced fracture extent and fault hydraulic conductivity were found to have a statistically significant impact on particle travel times, all with probabilities of not having zero effect of >0.9995. The most important of these three significant factors (as measured by ω^2) was the Collyhurst Sandstone. The Collyhurst Sandstone factor explained 14% of the original variance while induced fracture extent and fault hydraulic conductivity factors each explained no more than 7% of the original variance. The presence of the Collyhurst Sandstone encouraged the horizontal movement of particles within itself, rather than the vertical passage of particles through it and toward the shallower aquifer. The mean particle travel time for models with the Collyhurst Sandstone absent was 9,581 years (Table 3). No particles reached the Sherwood Sandstone in any scenarios where the Collyhurst Sandstone was present, hence the mean travel time of 15,000 years (the arbitrary limit chosen for ANOVA).

As for the fault hydraulic conductivity, no scenarios with the high value for fault hydraulic conductivity (10^{-4} m s^{-1}) resulted in particles reaching the Sherwood Sandstone (mean travel time of 15,000 years). The scenarios with medium (10^{-8} m s^{-1}) and low (10^{-12} m s^{-1}) fault hydraulic conductivities had mean travel times of 11,304 and 10,567 years, respectively. The post hoc Tukey tests on the levels of this factor showed that the significant difference lay between the highest value of the fault hydraulic conductivity and the other two levels but not between the medium and lower levels, i.e., it was when the fault was more conductive than the surrounding strata that it prevented upward particle travel. Less conductive faults led to the compartmentalization of hydraulic head and consequently encouraged the movement of particles vertically.

None of the scenarios without fracking or fluid injection resulted in particles reaching the Sherwood Sandstone, resulting in mean travel times of 15,000 years. The scenarios with induced fracture extents of 200 and 600 m had mean travel times of 11,381 and 10,490 years, respectively. That a greater induced fracture extent results in a shorter mean travel time to the Sherwood Sandstone is an intuitive result, but it should be emphasized that Davies et al. (2012) only reported a $\sim$5% chance of induced fractures propagating more than 200 m. Post hoc analysis of the induced fracture extent factor showed that the significant differences between levels of the factor were between the 0 m and both the 200 and 600 m induced fracture extents, but not between fracture extents of 200 and 600 m.

The horizontal head gradient and Manchester Marl were statistically insignificant factors, with probabilities of the factor having zero effect on the particle travel time of 0.855 and 0.243, respectively. That is, this study could find no statistical evidence that the low hydraulic conductivity Manchester Marl provided protection for the overlying aquifer. Rather it was the presence of higher hydraulic conductivity strata (i.e., the Collyhurst Sandstone) that led to greater fluid dispersion and therefore lent protection to overlying layers. Mean travel times for all factors are shown in Table 3.

3.2. Factor Interactions

The following factor interactions were all statistically significant (all with probabilities of not having zero effect of >0.9995): induced fracture extent with fault hydraulic conductivity, induced fracture extent with Collyhurst Sandstone, and fault hydraulic conductivity with Collyhurst Sandstone. The most important of the significant interactions (as measured by ω^2) was the interaction of the induced fracture extent with fault hydraulic conductivity. This interaction explained 42% of the original variance. The other significant interaction terms explained no more than 7% of the original variance. The shortest mean travel time for induced fracture extent with fault hydraulic conductivity interactions was 8,011

Table 3
Mean Travel Times With Standard Error for Factors and Statistically Significant Factor Interactions in the Initial Factorial Analysis

Factor or factor interaction	*P* value	Factor options		Mean (years)	Standard error of mean (years)
Collyhurst Sandstone	>0.9995	Absent		9,581	292
		Present		15,000	292
Induced fracture extent	>0.9995	0 m		15,000	358
		200 m		11,381	358
		600 m		10,490	358
Fault hydraulic conductivity	>0.9995	10^{-4} m s^{-1}		15,000	358
		10^{-8} m s^{-1}		11,304	358
		10^{-12} m s^{-1}		10,567	358
Horizontal head gradient	0.145	Absent		12,250	314
		Present		12,331	314
Manchester Marl	0.757	Absent		12,028	314
		Present		12,553	314
Induced fracture extent with Fault hydraulic conductivity	>0.9995	0 m	10^{-4} m s^{-1}	15,000	620
		0 m	10^{-8} m s^{-1}	15,000	620
		0 m	10^{-12} m s^{-1}	15,000	620
		200 m	10^{-4} m s^{-1}	15,000	620
		200 m	10^{-8} m s^{-1}	10,453	620
		200 m	10^{-12} m s^{-1}	8,690	620
		600 m	10^{-4} m s^{-1}	15,000	620
		600 m	10^{-8} m s^{-1}	8,460	620
		600 m	10^{-12} m s^{-1}	8,011	620
Induced fracture extent with Collyhurst Sandstone	>0.9995	0 m	Absent	15,000	506
		0 m	Present	15,000	506
		200 m	Absent	7,762	506
		200 m	Present	15,000	506
		600 m	Absent	5,981	506
		600 m	Present	15,000	506
Collyhurst Sandstone with Fault hydraulic conductivity	>0.9995	Absent	10^{-4} m s^{-1}	15,000	506
		Present	10^{-4} m s^{-1}	15,000	506
		Absent	10^{-8} m s^{-1}	7,608	506
		Present	10^{-8} m s^{-1}	15,000	506
		Absent	10^{-12} m s^{-1}	6,134	506
		Present	10^{-12} m s^{-1}	15,000	506

Note. P Value is the probability of a factor or interaction not having zero effect, judged at 95% confidence.

years, which occurred for scenarios with 600 m fractures and a fault hydraulic conductivity of 10^{-12} m s^{-1}. The shortest mean travel time for induced fracture extent with Collyhurst Sandstone interactions was 5,981 years, which occurred for scenarios with 600 m fractures and no Collyhurst Sandstone present. The shortest mean travel time for fault hydraulic conductivity with Collyhurst Sandstone interactions was 6,134 years, which occurred for scenarios with a fault hydraulic conductivity of 10^{-12} m s^{-1} and no Collyhurst Sandstone present. Mean travel times for all the statistically significant interactions are shown in Table 3. Seven of the possible 10 factor interactions were statistically insignificant (Table 4). The horizontal head gradient and Manchester Marl do not interact with other factors in a statistically significant way, further supporting the single factor results that they do not influence particle travel times to the Sherwood Sandstone.

Table 4
Insignificant Factor Interactions With Probabilities (P Value) of not Having Zero Effect, Judged at 95% Confidence

Factor interaction	*P* value
Induced fracture extent with Manchester Marl	0.368
Induced fracture extent with Horizontal head gradient	0.023
Fault hydraulic conductivity with Manchester Marl	0.475
Fault hydraulic conductivity with Horizontal head gradient	0.028
Manchester Marl with Collyhurst Sandstone	0.757
Manchester Marl with Horizontal head gradient	0.088
Collyhurst Sandstone with Horizontal head gradient	0.145
Overpressure with Induced fracture extent	0.720
Overpressure with Fault hydraulic conductivity	0.721

To test the effect of allocating an arbitrary 15,000 year travel time to scenarios where particles did not reach the Sherwood Sandstone within 10,000 years, the arbitrary travel time was changed to 10,000 and the ANOVA rerun with all the same factors and interactions as

before. The change in the default travel time made no difference to which factors and interactions were and were not significant at probability of 95% difference from zero. The proportion of the overall variance explained did shift marginally from 91.8% when 15,000 years was used compared to 89.9% when 10,000 years was used.

3.3. Overpressure

The significance of overpressure as a vulnerability factor was assessed using a further factorial analysis based on the results of the previous factorial analysis. Overpressure was a statistically significant factor with a probability of not having zero effect on the particle travel time of 0.966. The overpressure factor explained 8% of the original variance in the second factorial analysis, which was less important than the Collyhurst Sandstone factor (21% of the original variance in the second factorial analysis) and both the induced fracture extent and the fault hydraulic conductivity factors (both explained 10% of the original variance in the second factorial analysis). The interaction between overpressure with the Collyhurst Sandstone was also statistically significant (probability of not having zero effect of 0.966). This interaction explained 8% of the original variance in the second factorial analysis. Scenarios with no Collyhurst Sandstone and 40% overpressure were more likely to result in particle travel to the Sherwood Sandstone than scenarios with 10% overpressure (four of nine scenarios compared to one of nine). The following interactions were statistically insignificant: overpressure with induced fracture extent, and overpressure with fault hydraulic conductivity (Table 4).

3.4. Worst-Case Scenario

The worst-case scenario used the maximum strata hydraulic conductivity values of Cai and Ofterdinger (2014) and the factor combination that produced the shortest travel time scenario (560 years) in the initial factorial analysis (600 m induced fractures, fault hydraulic conductivity of 10^{-12} m s^{-1}, no Manchester Marl present, no Collyhurst Sandstone present, and no horizontal head gradient present). The particle travel time to the base of the Sherwood Sandstone for the worst-case scenario was 130 years (Figure 5). This was 430 years earlier than the equivalent scenario using typical strata hydraulic conductivity values.

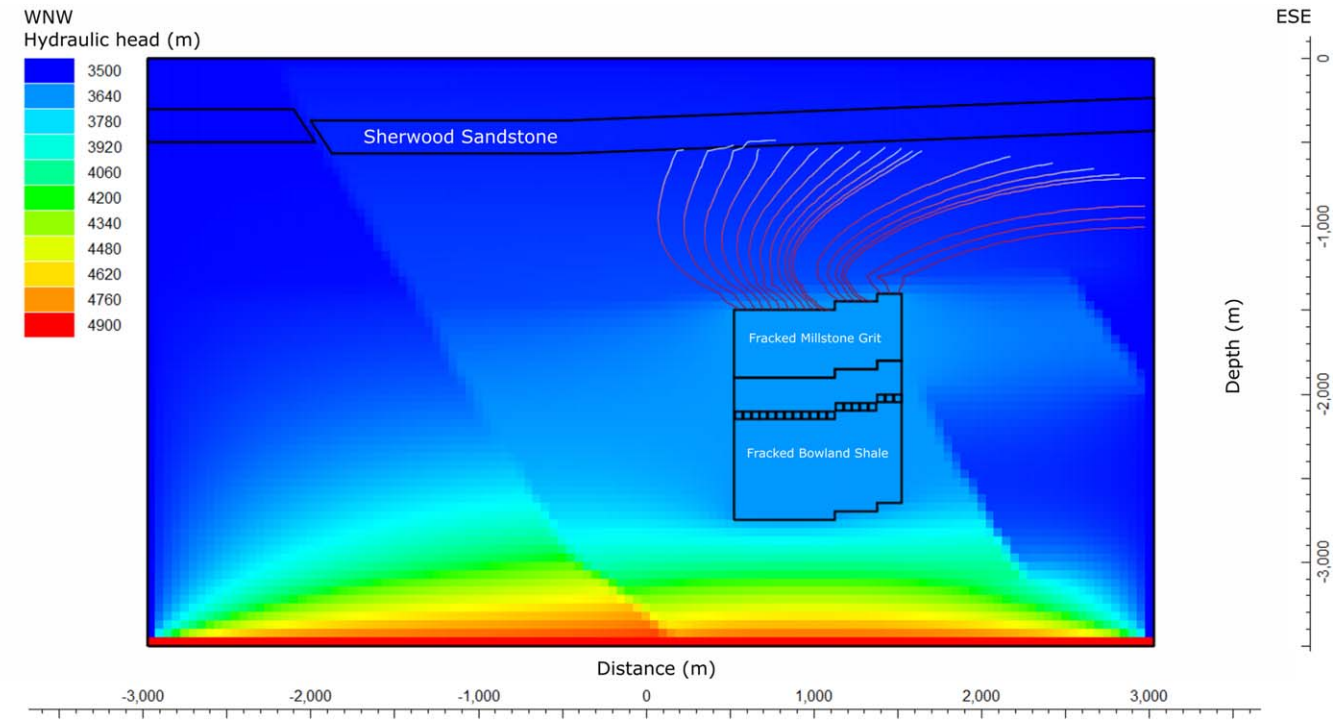

Figure 5. Simulated hydraulic head 10,000 years after the termination of fracking fluid injection in the worst-case scenario. Also shown are 130 year particle tracks (red to white graded curves), the Sherwood Sandstone, the fracked area (split by strata type), and stage locations.

4. Discussion

4.1. Induced Fracture Extent

No nonfractured scenarios resulted in particles reaching the base of the Sherwood Sandstone within 10,000 years but eight scenarios with a fracture extent of 200 m and eight scenarios with a fracture extent of 600 m did (Table 2). The majority of scenarios with 600 m fractures (six of eight) resulted in quicker travel times to the Sherwood Sandstone than the 200 m fracture scenarios (Table 2). This suggests that given certain hydrogeological configurations, the propagation of vertical fractures at the proposed site would increase the chance of fluid migration from the Bowland Shale to the Sherwood Sandstone. It also suggests that a greater induced fracture extent further increases the chance of fluid migration to the Sherwood Sandstone. However, 600 m induced vertical fractures are longer than any observed using microseismic data ($\sim$588 m) and the probability that an upward propagating fracture extends further than 200 m is $\sim$5% (Davies et al., 2012, see their Figure 6b). The difference in mean travel times for scenarios with 200 and 600 m induced fractures was 891 years with both means being of the order of 10,000 years (Table 3).

4.2. Faulting and Fault Hydraulic Conductivity

Environmental concerns related to faults and the migration of fracking fluids are generally focused on faults acting as fluid conduits to shallow aquifers (e.g., Gassiat et al., 2013; Myers, 2012). The results here suggest that the Haves Ho fault, which occurs at the land surface near the proposed site, will not act as a direct conduit for fracking fluid between the Bowland Shale and the Sherwood Sandstone, even when it is assigned a hydraulic conductivity higher than the most hydraulically conductive strata in the model. An explanation is that this is due to the interaction between the Haves Ho fault and the modeled overpressure. In the high hydraulic conductivity fault scenarios the Haves Ho fault acts to increase the hydraulic head values along its length to values higher than those at similar depths in the surrounding strata. This interaction results in a horizontal head gradient larger than the modeled regional horizontal head gradient and the movement of particles horizontally away from the fault. When the modeled faults are assigned low values for hydraulic conductivity, the scenarios display pressure compartmentalization (hydraulic heads increase in the area between the Haves Ho fault and Fault-1, see Figure 5 for an example). Pressure compartmentalization discourages horizontal fluid migration (the faults act as barriers to horizontal groundwater flow) and encourages vertical fluid migration, resulting in scenarios with upward particle migration to the Sherwood Sandstone. Because faults are a common element of sedimentary basins, this modeling result is important in aquifer-vulnerability assessments. The pressure-compartmentalization effects of low hydraulic conductivity faults mean that low hydraulic conductivity faults may, in some hydrogeological scenarios, lead to greater shallow aquifer vulnerability than the presence of high hydraulic conductivity faults.

4.3. Low and High Hydraulic Conductivity Stratigraphic Barriers

The low hydraulic conductivity Manchester Marl, which was expected to act as the key vertical migration barrier (Ove Arup and Partners Ltd., 2014a), was not a statistically significant factor (probability of having zero effect of 0.243). Cai and Ofterdinger (2014) concluded that the high hydraulic conductivity Collyhurst Sandstone acts as a significant barrier to upward fluid migration by increasing horizontal fluid flux. Our results support this conclusion. All scenarios where particles reached the Sherwood Sandstone within 10,000 years had the Collyhurst Sandstone absent. Additionally, no scenarios where the Collyhurst Sandstone was present resulted in vertical migration to the Sherwood Sandstone within 10,000 years. In contrast to Cai and Ofterdinger (2014), horizontal flow in the modeled Collyhurst Sandstone is reversed to the regional horizontal head gradient, highlighting the importance of stratigraphic interactions with faults and overpressure. These results indicate that high hydraulic conductivity formations in the deep subsurface, but beyond the induced fracture extent, can be more effective barriers to upward fluid migration than low hydraulic conductivity formations. Numerical modeling of the North German Basin also showed horizontal fluid transport in more hydraulically conductive formations above the modeled fluid injection (Pfunt et al., 2016), suggesting that this protective mechanism is not unique to the proposed site.

4.4. Overpressure

An overpressured formation is one in which the pore fluids contained within it are at a higher pressure than the hydrostatic pressure for that depth. One mechanism of overpressure formation is disequilibrium compaction; sediment is buried quicker than its pore water can escape. The conditions that favor disequilibrium

compaction are rapid burial and low permeability, thus many shale successions with their low permeability and often rapid burial are commonly overpressured. Furthermore, the conversion of kerogen to oil and gas may be accompanied by volume expansion. Within a closed or low permeability system this can also contribute to overpressure (Osborne & Swarbrick, 1997). Various shale resources around the globe are overpressured (EIA, 2011; Gassiat et al., 2013 and references therein). Overpressure was found to be a statistically significant factor in this study. Furthermore, the interaction of overpressure with the Collyhurst Sandstone was also statistically significant. When the Collyhurst Sandstone was not present, the scenarios with 40% overpressure were more likely to result in particle travel to the Sherwood Sandstone within 10,000 years than scenarios with 10% overpressure, i.e., a greater upward driving force resulted in a quicker travel time. When the Collyhurst Sandstone was present, the magnitude of the overpressure made no difference to the travel time to the Sherwood Sandstone (particles did not reach the Sherwood Sandstone within 10,000 years). This result occurred because particles were transported horizontally within the Collyhurst Sandstone as a result of induced horizontal head gradients greater than the modeled regional horizontal head gradient. Given the common occurrence of overpressure in shale resources, its possible presence and magnitude should be considered along with overlying stratigraphy and geological structure when assessing shallow aquifer vulnerability.

4.5. Shallow Aquifer Vulnerability

The vulnerability of shallow aquifers to anthropogenically introduced fluids has generally concentrated on fluids introduced at the surface, for example, the potential pollution by agricultural pesticides (e.g., Worrall & Kolpin, 2004) or chemical spills (e.g., Gross et al., 2013). Subsurface fracking operations introduce a new potential source of aquifer contamination. Because such operations in England would inject fluids into shales at a minimum depth of 1,000 m by law, shallow aquifer vulnerability must now also be considered from a bottom-up perspective. We have identified important factors to consider in a bottom-up approach to shallow aquifer vulnerability at proposed fracking sites: the vertical extent of induced fractures, the magnitude of overpressure, the presence of high hydraulic conductivity formations acting as vertical fluid barriers, and low hydraulic conductivity faults leading to pressure compartmentalization. The latter two factors are not normally considered (e.g., Ove Arup and Partners Ltd., 2014a), but the results of this study suggest that they should be factors to consider in shallow aquifer vulnerability at proposed fracking sites.

4.6. Model Limitations

4.6.1. 2-D Versus 3-D Models

The modeled scenarios in this study were all 2-D because of the single geological cross section available. This approach restricts the flow directions within the model to the 2-D plane. This necessary restriction may influence particle travel times by not allowing lateral movement of the particles. To investigate any lateral flow effects on travel times, the model domain was extended by 1,000 m to the north-northeast and south-southwest (Figure 6), i.e., the 3-D model had a width of 2,050 m (note that the original 2-D model had a width of 50 m but was essentially 2-D in comparison to the length and depth scales). SRVs were assumed to have the same horizontal extent as the vertical extent. The model was not made any wider than 2,050 m because the 3-D geology in the area is uncertain. However, it is wide enough to accommodate 600 m fractures and exclude edge effects. Scenarios were not run in 3-D for every 2-D scenario because of time constraints setting up the 3-D versions. Instead, five 3-D simulations were chosen based on their factor combinations (Table 5).

The extension to 3-D had no effect on the particle travel time in the worst-case scenario, however ~75 m of lateral movement was observed by the time the particles reached the base of the Sherwood Sandstone (Table 5). Lateral particle movement was also observed for three other scenarios. Two of these had the Collyhurst Sandstone absent. In these scenarios, travel times increased by 70 and 280 years, equating to ~13% and ~16% increases in respective travel times (Table 5). When the Collyhurst Sandstone was present extensive lateral movement was observed and particles reached the eastern corner of the 3-D model domain. However, particles remained within the Collyhurst Sandstone and did not reach the Sherwood Sandstone aquifer, supporting the 2-D scenario results that the Collyhurst Sandstone acts as an effective barrier to upward flow. The remaining scenario, with high fault hydraulic conductivity (10^{-4} m s^{-1}), showed no lateral movement in the 3-D scenario and particles did not reach the Sherwood Sandstone (Table 5).

While lateral movement of particles is sometimes observed when the 2-D scenarios are run in 3-D, the travel time results still support the 2-D results that the Collyhurst Sandstone acts as an upward flow barrier and

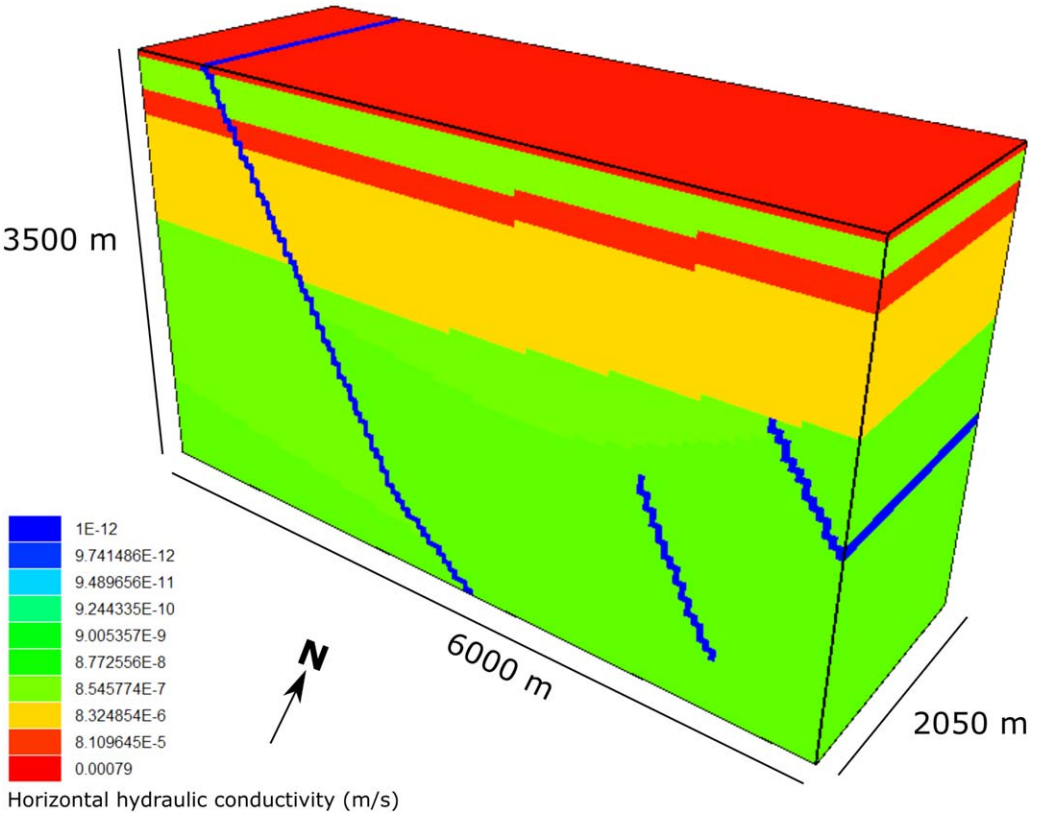

Figure 6. 3-D model domain using strata hydraulic conductivities from the worst-case scenario. The SRV is situated in the middle of the model and hidden from view.

low hydraulic conductivity faults encourage vertical fluid flow by developing subsurface pressure compartmentalization. Furthermore, the extension to 3-D can increase travel times to aquifers, thereby reducing aquifer contamination risk. As more information and data are released for this study area, the development of more informed, more extensive, and more sophisticated 3-D models will be possible to further investigate these results.

4.6.2. Particle Use and Assumptions

In each scenario, particles were released at the edge of the SRV because fracture propagation was not modeled explicitly. However, it is unclear in practice if injected fluid always reaches the edge of the SRV. To investigate the travel time sensitivity to initial particle placement, six further 2-D models were run under the same hydraulic conditions as the worst-case scenario. These six scenarios decreased the distance between the injection cells and the particle release point at intervals of 100 m (the SRV remained at 600 m extent).

Table 5
Particle Travel Times and Extent of Lateral Movement for 3-D Scenarios

Induced fracture extent (m)	Fault hydraulic conductivity (m s^{-1})	Collyhurst Sandstone present?	Travel time to nearest 10 years	Travel time difference compared to 2-D scenario (years)	Approximate extent of lateral movement (m)
600	10^{-12}	No	130*	0	75
600	10^{-12}	No	630	+70	50
600	10^{-4}	No	10,000	0	0
600	10^{-12}	Yes	10,000	0	1000
200	10^{-12}	No	2,040	+280	175

Note. The Manchester Marl and horizontal head gradient were absent in all scenarios.
* is the worst-case scenario of section 3.4.
+ indicates an increase in particle travel time compared to the equivalent 2-D scenario.

Table 6
Particle Travel Times for the Worst-Case Scenario With Particles Released at Different Distances From the Injection Cells

Distance between injection cells and particle release point (m)	Travel time to nearest 10 years
600*	130
500	130
400	130
300	130
200	140
100	140
0	140

Note. * is the original worst-case scenario of section 3.4.

Travel times for distances ≥300 m were the same as the original worst-case scenario and 10 years greater for distances ≤200 m (Table 6). Although the travel times were slightly greater for release points ≤200 m to the injection cells, the effect does not substantially increase travel times, suggesting that the model results were not very sensitive to initial particle placement within the SRV.

The study used the travel times of the first particles to reach the base of the Sherwood Sandstone as a measure of contamination risk. Chemical concentrations, which would be the common measure for comparison with environmental standards in aquifers and surface waters, were not considered. In reality, fracking fluids passing through geological strata would be subject to a number of natural attenuation processes, which could include nonconservative processes such as dilution, dispersion, degradation, adsorption, and precipitation. Such processes would decrease, remove, and/or retard the fracking fluid constituents and contribute to increasing the travel time to shallow aquifers. In addition, all the constituents of a fracking fluid are subject to chemical risk assessments. In England only substances determined as "nonhazardous" by the Environment Agency have been identified suitable for permits. However, a major water quality concern from shale exploitation is the highly saline nature of fracking and flowback fluids, and salinity is generally a conservative property in water bodies. Nevertheless, at the proposed site in this study the shallow regional aquifer is expected to be saline and is not currently used as a groundwater resource (Griffiths et al., 2003; Sage & Lloyd, 1978).

4.6.3. Operational Effects

Variations in the fracking operation parameters were not considered in the scenarios. A single injection rate and a consistent number of fracking stages were used in all models. These values may be different to the proposed fracking operation if it goes ahead, although they are likely to be similar. Another operational aspect to note is that modeled fluid injection was run simultaneously for all stages without flowback. A real fracking operation would inject stage fluids sequentially, flow back fluids between each stage, and then ideally produce hydrocarbons for a number of years. Flowback and production decrease the pressure and volume of fluid in the subsurface, reducing the chances of fluid migration into the overburden. Birdsell et al. (2015) included flowback and production in their numerical model and found that, in scenarios with a permeable pathway to the shallow aquifer, the combined effect of production and capillary imbibition reduced the amount of fracking fluid reaching the aquifer by a factor of 10. Brownlow et al. (2016) also studied the effect of flowback and production as part of a numerical model investigating the influence of fracking operations on abandoned or converted boreholes. The flowback of 8% of the injected fluid volume had negligible effect to head values. However, production over 15 years reduced head values to nominal values up to 200 m from the fracked borehole (Brownlow et al., 2016).

To investigate the particle travel time sensitivity to flowback and production, the same 15 year flowback and production scenario of Brownlow et al. (2016) was employed to our worst-case scenario (Table 7). Particles were released at the upper edge of the SRV on the termination of injection. Each fracking injection stage of the model commenced flowback and production following the termination of injection using the Well package (WEL) within ModelMuse and MODFLOW. Despite the inclusion of flowback and production, particles reached the base of the Sherwood Sandstone in 130 years; the same as the original worst-case scenario. The key difference between this scenario and that by Brownlow et al. (2016) is the simulation time. Our scenario had a simulation time 10,000 years beyond the 15 year production phase, whereas Brownlow et al. (2016) ended their simulation after 15 years of production. Consequently, the 130 year travel time is the result of the long-term interaction of the SRV and the model boundary conditions, which dominate over the shorter production phase. However, it is recognized that the model in this study does not account for fracture aperture reduction and subsequent hydraulic conductivity reduction associated with production from a SRV (Birdsell et al., 2015).

Table 7
Time Phases for the Flowback and Production Scenario

Time phase	Time interval	Approximate fluid injection/extraction rate ($m^3 s^{-1}$)
Steady state	30 years	0
Fluid injection	2 h	+0.35
Flowback	7 days	−0.00033
Early production	2 years	−0.00019
Main production	13 years	−0.00004
Post production	10,000 years	0

Note. + and − indicate fluid injection and extraction, respectively.

4.6.4. Other Effects

The cross section used in this study is based on confidential seismic interpretation, which inherently introduces errors. For example, the tops of formations may have been interpreted at the wrong two-way-time, time to depth conversion may have been inaccurate, and faults may have been incorrectly placed or missed due to the seismic resolution. Another model limitation was the availability of hydraulic data. While shallow groundwater flow has been modeled effectively to the east of the proposed site (MacDonald, 1997), little is known about the hydraulic properties and gradients of the deep strata in the Bowland Basin. Future data from deep borehole core samples and pumping tests would help constrain the model parameters.

The effects of heat, variable-density flow, and multiphase flow were not modeled. Thermal and density gradients in the subsurface can lead to the advection of groundwater. These effects could enhance or inhibit the migration of fracking fluids depending on the particular hydrogeological scenario. Multiphase flow could be an important factor to model in future studies because fracking fluid injection leads to at least two-phase flow within a shale gas reservoir (injected liquid water and chemicals, injected solid proppants, and in situ natural gas—phase dependent on subsurface pressure). With the introduction of multiple phases, the absolute permeability of a single phase is reduced to the effective permeability. This decrease in permeability would reduce the ability of fracking fluid to flow through, and potentially out of, the shale reservoir.

A final remark is that Davies et al. (2012) based their induced fracture extents on microseismic data, which may not record the full extent of stimulated fractures (Lacazette & Geiser, 2013). Stimulated fractures beyond the fractures mapped from microseismic data may extend the SRV beyond the considered maximum limit of 600 m, which may reduce particle travel times.

5. Conclusions

A proposed hydraulic fracturing operation in a sedimentary basin with complex geological structure was numerically modeled to identify statistically significant hydrogeological factors which increase the vulnerability of shallow groundwater resources. Under certain hydrogeological configurations, fracking of the shale resource at ~2,000 m below the surface decreased the travel time of fluid migration between the shale formation and the shallow regional aquifer at ~300–500 m below the surface. Of the 91 modeled hydrogeological scenarios, 18 scenarios resulted in particle travel times to the shallow aquifer within 10,000 years. The study found that four subsurface factors acted to decrease particle travel times to the shallow aquifer and as a result increased the vulnerability of that groundwater resource:

1. increased induced fracture extent,
2. low hydraulic conductivity faults, which result in pressure compartmentalization and encourage vertical fluid migration,
3. the absence of deep high hydraulic conductivity formations above the greatest induced fracture extent,
4. and greater amounts of overpressure.

These factors in shale basins could lead to the vulnerability of shallow aquifers from fracking fluids injected at several kilometers depth. Two factors are not typically considered in shale exploitation environmental risk assessments: deep high hydraulic conductivity formations above the greatest induced fracture extent can be more effective barriers to vertical fluid flow than low hydraulic conductivity formations, and low hydraulic conductivity faults can encourage vertical fluid migration more than high hydraulic conductivity faults. The worst-case scenario modeled, which uses an unlikely hydrogeological configuration at the proposed site and induced vertical fractures greater than ever observed using microseismic data, resulted in a travel time to the shallow aquifer of 130 years. This result does not account for dilution, dispersion, degradation, adsorption or precipitation of the fracking fluid constituents, which would all act to increase the travel time.

Acknowledgments

This research was funded by a Durham Doctoral Studentship awarded to Miles Wilson. It is part of the research carried out by the Researching Fracking (ReFINE) consortium led by Newcastle and Durham Universities, but no funding was received from this body for this study. We thank Scott James and one anonymous reviewer for their constructive critique of the original manuscript, which greatly enhanced the discussion of the model. Richard Winston of the USGS is also thanked for his help with ModelMuse. All data used in the numerical modeling are stated within the text. MODFLOW, ModelMuse and MODPATH are all open-access software available from the USGS.

References

Allen, D. J., Brewerton, L. J., Coleby, L. M., Gibbs, B. R., Lewis, M. A., MacDonald, A. M., . . . Williams, A. T. (1997). *The physical properties of major aquifers in England and Wales* (Brit. Geol. Surv. Tech. Rep. WD/97/34, 312 p.). Bristol, UK: Environment Agency.

Ambrose, K., Hough, E., Smith, N. J. P., & Warrington, G. (2014). *Lithostratigraphy of the Sherwood sandstone group of England, Wales and south-west Scotland* (Brit. Geol. Surv. Res. Rep. RR/14/01). Keyworth, Nottingham, UK: British Geological Survey.

Andrews, I. J. (2013). *The Carboniferous Bowland Shale gas study: Geology and resource estimation*. London, UK: British Geological Survey for the Department of Energy and Climate Change.
Belcher, W. R., & Sweetkind, D. S. (2010). Death Valley regional groundwater flow system, Nevada and California: Hydrogeologic framework and transient groundwater flow model (U.S. Geol. Surv. Prof. Pap. 1711, 398 p.). Reston, VA: U.S. Geological Survey.
Birdsell, D. T., Rajaram, H., Dempsey, D., & Viswanathan, H. S. (2015). Hydraulic fracturing fluid migration in the subsurface: A review and expanded modeling results. *Water Resources Research*, *51*, 7159–7188. https://doi.org/10.1002/2015WR017810
Boothroyd, I. M., Almond, S., Worrall, F., & Davies, R. J. (2017). Assessing the fugitive emission of CH_4 via migration along fault zones—Comparing potential shale gas basin to non-shale basins in the UK. *Science of the Total Environment*, *580*, 412–424.
Brownlow, J. W., James, S. C., & Yelderman, J. C. (2016). Influence of hydraulic fracturing on overlying aquifers in the presence of leaky abandoned wells. *Ground Water*, *54*(6), 781–792.
Brownlow, J. W., Yelderman, J. C., & James, S. C. (2017). Spatial risk analysis of hydraulic fracturing near abandoned and converted oil and gas wells. *Ground Water*, *55*(2), 268–280.
Cai, Z., & Ofterdinger, U. (2014). Numerical assessment of potential impacts of hydraulically fractured Bowland Shale on overlying aquifers. *Water Resources Research*, *50*, 6236–6259. https://doi.org/10.1002/2013WR014943
Clancy, S. A., Worrall, F., Davies, R. J., & Gluyas, J. G. (2017). An assessment of the footprint and carrying capacity of oil and gas well sites: The implications for limiting hydrocarbon resources. *Science of the Total Environment*. https://doi.org/10.1016/j.scitotenv.2017.02.160
Clarke, H., Bustin, M., & Turner, P. (2014, February), Unlocking the Resource Potential of the Bowland Basin, NW England, paper presented at *SPE/EAGE European Unconventional Resources Conference and Exhibition*. Vienna, Austria: Society of Petroleum Engineers.
Cohen, H. A., Parratt, T., & Andrews, C. B. (2013). Potential contaminant pathways from hydraulically fractured shale to aquifers. *Groundwater*, *51*(3), 317–319.
Davies, R. J., Almond, S., Ward, R. S., Jackson, R. B., Adams, C., Worrall, F., Herringshaw, L. G., Gluyas, J. G., & Whitehead, M. A. (2014). Oil and gas wells and their integrity: Implications for shale and unconventional resource exploitation. *Marine and Petroleum Geology*, *56*, 239–254.
Davies, R. J., Foulger, G., Bindley, A., & Styles, P. (2013). Induced seismicity and hydraulic fracturing for the recovery of hydrocarbons. *Marine and Petroleum Geology*, *45*, 171–185.
Davies, R. J., Mathias, S. A., Moss, J., Hustoft, S., & Newport, L. (2012). Hydraulic fractures: How far can they go? *Marine and Petroleum Geology*, *37*(1), 1–6.
DiGiulio, D. C., Wilkin, R. T., Miller, C., & Oberley, G. (2011). *Investigation of ground water contamination near Pavillion, Wyoming* (EPA 600/R-00/000). Ada, OK: Office of Research and Development, National Risk Management Research Laboratory.
EIA (2011). *World shale gas resources: An initial assessment of 14 regions outside the United States* (report, 365 pp.). Washington, DC: U.S. Department of Energy.
Environment Agency (EA) (2013). *An environmental risk assessment for shale gas exploratory operations in England* (LIT 8474), Bristol, UK: Environment Agency.
Fisher, M. K., & Warpinski, N. R. (2012). Hydraulic-fracture-height growth: Real data. *SPE Production & Operations*, *27*(1), 8–19.
Fisher, Q. J., & Knipe, R. J. (2001). The permeability of faults within siliciclastic petroleum reservoirs of the North Sea and Norwegian Continental Shelf. *Marine and Petroleum Geology*, *18*(10), 1063–1081.
Flewelling, S. A., & Sharma, M. (2014). Constraints on upward migration of hydraulic fracturing fluid and brine. *Ground Water*, *52*(1), 9–19.
Gaskari, R., & Mohaghegh, S. D. (2006, January), Estimating major and minor natural fracture pattern in gas shales using production data, paper presented at *SPE Eastern Regional Meeting*, Canton, OH: Society of Petroleum Engineers.
Gassiat, C., Gleeson, T., Lefebvre, R., & McKenzie, J. (2013). Hydraulic fracturing in faulted sedimentary basins: Numerical simulation of potential contamination of shallow aquifers over long time scales. *Water Resources Research*, *49*, 8310–8327. https://doi.org/10.1002/2013WR014287
Green, C. A., Styles, P., & Baptie, B. J. (2012). *Preese Hall shale gas fracturing review and recommendations for induced seismic mitigation*. London, UK: Department of Energy and Climate Change.
Griffiths, K. J., Shand, P., & Ingram, J. (2003). *Baseline Report Series: 8. The Permo-Triassic sandstones of Manchester and East Cheshire* (Brit. Geol. Surv. Commiss. Rep. CR/03/265N). Keyworth, Nottingham, UK: British Geological Survey.
Gross, S. A., Avens, H. J., Banducci, A. M., Sahmel, J., Panko, J. M., & Tvermoes, B. E. (2013). Analysis of BTEX groundwater concentrations from surface spills associated with hydraulic fracturing operations. *Journal of the Air & Waste Management Association*, *63*(4), 424–432.
Harbaugh, A. W. (2005). *MODFLOW-2005, The U.S. Geological Survey modular ground-water model: The ground-water flow process*. (U.S. Geol. Surv. Tech. Methods 6-A16, variously p.). Reston, VA: U.S. Geological Survey.
Hird, C., & Clarke, H. (2012). *Permeability and Stress Sensitivity Analysis Preese Hall-1 (CBM Solutions)* (Cuadrilla Resources Preese Hall-1 end of well report LJ/06-5, 795 p.). Bamber Bridge, Lancashire, UK: Cuadrilla Resources Ltd.
Kahrilas, G. A., Blotevogel, J., Stewart, P. S., & Borch, T. (2014). Biocides in hydraulic fracturing fluids: A critical review of their usage, mobility, degradation, and toxicity. *Environmental Science & Technology*, *49*(1), 16–32.
King, G. E. (2012, January), Hydraulic fracturing 101: What every representative, environmentalist, regulator, reporter, investor, university researcher, neighbor and engineer should know about estimating frac risk and improving frac performance in unconventional gas and oil wells, paper presented at *SPE Hydraulic Fracturing Technology Conference*. The Woodlands, TX: Society of Petroleum Engineers.
Kissinger, A., Helmig, R., Ebigbo, A., Class, H., Lange, T., Sauter, M., . . . Jahnke, W. (2013). Hydraulic fracturing in unconventional gas reservoirs: Risks in the geological system, part 2. *Environmental Earth Sciences*, *70*(8), 3855–3873.
Lacazette, A., & Geiser, P. (2013). Comment on Davies et al., 2012—Hydraulic fractures: How far can they go? *Marine and Petroleum Geology*, *43*, 516–518.
Llewellyn, G. T., Dorman, F., Westland, J. L., Yoxtheimer, D., Grieve, P., Sowers, T., . . . Brantley, S. L. (2015). Evaluating a groundwater supply contamination incident attributed to Marcellus Shale gas development. *Proceedings of the National Academy of Sciences of United States of America*, *112*(20), 6325–6330.
MacDonald, M. (1997). Fylde aquifer/Wyre catchment water resources study (Final Rep. 38436BA01/2/C TOC). Bristol, UK: Environment Agency.
Mayerhofer, M. J., Lolon, E., Warpinski, N. R., Cipolla, C. L., Walser, D. W., & Rightmire, C. M. (2010). What is stimulated reservoir volume? Paper presented at *SPE Shale Gas Production Conference*, Fort Worth, Texas.
McDonald, M. G., & Harbaugh, A. W. (1984). *A modular three-dimensional finite-difference ground-water flow model* (U.S. Geol. Surv. Open File Rep. 83–875, 528 p.). Reston, VA: U.S. Geological Survey.
Myers, T. (2012). Potential contaminant pathways from hydraulically fractured shale to aquifers. *Ground Water*, *50*(6), 872–882.
Olejnik, S., & Algina, J. (2003). Generalized eta and omega squared statistics: Measures of effect size for some common research designs. *Psychological Methods*, *8*(4), 434–447.

Osborne, M. J., & Swarbrick, R. E. (1997). Mechanisms for generating overpressure in sedimentary basins: A reevaluation. *AAPG Bulletin*, *81*(6), 1023–1041.

Ove Arup and Partners Ltd. (2014a). *Environmental statement temporary Shale gas extraction Preston New Road, Lancashire* (PNR_ES_Vol1_Environmental Statement). Cuadrilla Bowland Ltd.

Ove Arup and Partners Ltd. (2014b). *Appendix L: Induced seismicity environmental statement temporary Shale Gas extraction Preston New Road, Lancashire* (PNR_ES_Vol2_Appndx L_Induced Seismicity). Cuadrilla Bowland Ltd.

Palat, S., Torbatynia, M., Kanadikirik, K., & Varma, S. (2015, November), Hydrodynamic modeling of hydraulic fracturing fluid injection in North Perth Basin Shale Gas Targets, paper presented at *SPE Asia Pacific Unconventional Resources Conference and Exhibition*. Brisbane, Australia: Society of Petroleum Engineers.

Palmer, R. C., & Lewis, M. A. (1998). Assessment of groundwater vulnerability in England and Wales. *Geological Society, London, Special Publications*, *130*(1), 191–198.

Pfunt, H., Houben, G., & Himmelsbach, T. (2016). Numerical modeling of fracking fluid migration through fault zones and fractures in the North German Basin. *Hydrogeology Journal*, *24*(6), 1343–1358.

Pollock, D. W. (2012). *User guide for MODPATH Version 6: A particle-tracking model for MODFLOW* (U.S. Geol. Surv. Tech. Methods 6-A41, 58 p.). Reston, VA: U.S. Geological Survey.

Rutqvist, J., Rinaldi, A. P., Cappa, F., & Moridis, G. J. (2013). Modeling of fault reactivation and induced seismicity during hydraulic fracturing of shale-gas reservoirs. *Journal of Petroleum Science and Engineering*, *107*, 31–44.

Rutqvist, J., Rinaldi, A. P., Cappa, F., & Moridis, G. J. (2015). Modeling of fault activation and seismicity by injection directly into a fault zone associated with hydraulic fracturing of shale-gas reservoirs. *Journal of Petroleum Science and Engineering*, *127*, 377–386.

Sage, R. C., & Lloyd, J. W. (1978). Drift deposit influences on the Triassic Sandstone aquifer of NW Lancashire as inferred by hydrochemistry. *Quarterly Journal of Engineering Geology and Hydrogeology*, *11*(3), 209–218.

Seymour, K. J., Ingram, J. A., & Gebbett, S. J. (2006). Structural controls on groundwater flow in the Permo-Triassic sandstones of NW England. *Geological Society, London, Special Publications*, *263*(1), 169–185.

UK Technical Advisory Group (UKTAG) (2011). *Defining and reporting on groundwater bodies* (Working Pap. Version V6.21/Mar/2011). Bristol, UK: Environment Agency. Retrieved from https://www.wfduk.org/stakeholders/uktag

United States Energy Information Administration (US EIA) (2016). *U.S. Shale production*. Retrieved from http://www.eia.gov/dnav/ng/hist/res_epg0_r5302_nus_bcfa.htm, accessed 24 April 2017

Vengosh, A., Warner, N., Jackson, R., & Darrah, T. (2013). The effects of shale gas exploration and hydraulic fracturing on the quality of water resources in the United States. *Procedia Earth and Planetary Science*, *7*, 863–866.

Wilson, M. P., Davies, R. J., Foulger, G. R., Julian, B. R., Styles, P., Gluyas, J. G., & Almond, S. (2015). Anthropogenic earthquakes in the UK: A national baseline prior to shale exploitation. *Marine and Petroleum Geology*, *30*(1), e17.

Winston, R. B. (2009). *ModelMuse—A graphical user interface for MODFLOW-2005 and PHAST* (U.S. Geol. Surv. Tech. Methods 6-A29, 52 p.). Reston, VA: U.S. Geological Survey.

Worrall, F., & Kolpin, D. W. (2004). Aquifer vulnerability to pesticide pollution—Combining soil, land-use and aquifer properties with molecular descriptors. *Journal of Hydrology*, *293*(1), 191–204.

Wright, P. R., McMahon, P. B., Mueller, D. K., & Clark, M. L. (2012). *Groundwater-quality and quality-control data for two monitoring wells near Pavillion, Wyoming, April and May 2012* (No. 718, pp. i-23). Reston, VA: U.S. Geological Survey.